Nat Hazards (2012) 64:593–614
DOI 10.1007/s11069-012-0259-5

ORIGINAL PAPER

Comparison of near-fault and far-fault ground motion effects on geometrically nonlinear earthquake behavior of suspension bridges

Süleyman Adanur · Ahmet Can Altunişik · Alemdar Bayraktar · Mehmet Akköse

Received: 8 June 2009 / Accepted: 14 June 2012 / Published online: 27 June 2012

Abstract This paper presents a comparison of near-fault and far-fault ground motion effects on geometrically nonlinear earthquake behavior of suspension bridges. Boğaziçi (The First Bosporus) and Fatih Sultan Mehmet (Second Bosporus) suspension bridges built in Istanbul, Turkey, are selected as numerical examples. Both bridges have almost the same span. While Boğaziçi Suspension Bridge has inclined hangers, Fatih Sultan Mehmet Suspension Bridge has vertical hangers. Geometric nonlinearity including P-delta effects from self-weight of the bridges is taken into account in the determination of the dynamic behavior of the suspension bridges for near-fault and far-fault ground motions. Near-fault and far-fault strong ground motion records, which have approximately identical peak ground accelerations, of 1999 Chi-Chi, 1999 Kocaeli, and 1979 Imperial Valley earthquakes are selected for the analyses. Displacements and internal forces of the bridges are determined using the finite element method including geometric nonlinearity. The displacements and internal forces obtained from the dynamic analyses of suspension bridges subjected to each fault effect are compared with each other. It is clearly seen that near-fault ground motions are more effective than far-fault ground motion on the displacements and internal forces such as bending moment, shear force and axial forces of the suspension bridges.

Keywords Suspension bridge · Far-fault ground motion · Near-fault ground motion · Geometric nonlinearity · Nonlinear earthquake behavior · P-delta effect

S. Adanur · A. C. Altunişik (✉) · A. Bayraktar · M. Akköse
Department of Civil Engineering, Karadeniz Technical University, 61080 Trabzon, Turkey
e-mail: ahmetcan8284@hotmail.com

S. Adanur
e-mail: sadanur@ktu.edu.tr

A. Bayraktar
e-mail: alemdar@ktu.edu.tr

M. Akköse
e-mail: akkose@ktu.edu.tr

1 Introduction

Near-fault ground motions recorded in recent major earthquakes (1999 Taiwan Chi-Chi, 1989 Loma Prieta, 1994 US Northridge, and 1995 Japan Hyogoken-Nanbu) are characterized by a ground motion with large velocity pulse, which exposes the structures to high input energy in the beginning of the earthquake. Comparison of the near-fault strong ground motion velocities with far-fault strong ground motions is shown in Fig. 1 (Akkar et al. 2005). These pulses are strongly influenced by the orientation of the fault, the direction of slip on the fault, and the location of the recording station relative to the fault which is termed as 'directivity effect' due to the propagation of the rupture toward the recording site (Archuleta and Hartzell 1981; Megawati et al. 2001; Agrawal and He 2002; Wang et al. 2002; Somerville 2003; Bray and Marek 2004; Pulido and Kubo 2004; Akkar et al. 2005).

The effects of near-fault ground motion on many civil engineering structures such as buildings, tunnels, dams, bridges, nuclear station have been investigated in many recent studies (Hall et al. 1995; Malhotra 1999; Ohmachi and Jalali 1999; Chopra and Chintanapakdee 2001; Rao and Jangid 2001; Liao et al. 2004; Corigliano et al. 2006; Galal and Ghobarah 2006; Ghahari et al. 2006; Dicleli and Buddaram 2007; Bayraktar et al. 2008). It can be clearly seen from these studies that the importance of near-fault ground motion effect on the response of the structures has been highlighted.

There are many studies about the dynamic responses of suspension bridges under the uniform or nonuniform earthquake ground motions using deterministic or stochastic methods in the literature (Abdel-Ghaffar 1976, 1980; Abdel-Ghaffar and Rubin 1982, 1983a, b, Abdel-Ghaffar and Stringfellow 1984; Dumanoğlu and Severn 1987, 1989, 1990; Dumanoğlu et al. 1992; Hyun et al. 1992; Nakamura et al. 1993; Brownjohn 1994; Harichandran et al. 1996; Rassem et al. 1996; Wang et al. 1999; Zhang et al. 2005). However, there is not sufficient research about the effects of near-fault ground motions on dynamic responses of suspension bridges.

Suspension bridges consist of elements like tower, cable, hanger and deck; the behavior of each one is different. Under the effect of external forces and self-weight of the bridge, especially cables and hangers are subjected to large tension forces, which have considerable influence on the element stiffness matrices. This characteristic is called as geometric nonlinearity of the structural elements and should be taken into account in the analysis of suspension bridges.

The main objective of this paper is to determine and compare the earthquake behavior of suspension bridge subjected to near-fault and far-fault ground motions considering geometric nonlinearity. For this purpose, Boğaziçi (The First Bosporus) suspension bridge

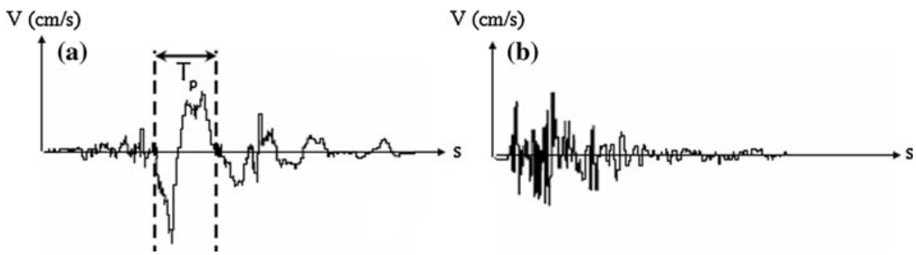

Fig. 1 The time-histories of strong ground motion velocities (Akkar et al. 2005). **a** Near-fault strong ground motion. **b** Far-fault strong ground motion

with inclined hangers and Fatih Sultan Mehmet (Second Bosporus) suspension bridge with vertical hangers are utilized. The 1999 Chi-Chi, 1999 Kocaeli, and 1979 Imperial Valley earthquake records are selected to represent the near-fault ground motion characteristics. In this study, the term "near-fault ground motion" is referred to the ground motion record obtained in the vicinity of a fault with apparent velocity pulse (pulse duration larger than 1.0 s), the distance of the fault of the ground motion record less than 10 km, and the peak ground velocity/peak ground acceleration (PGV/PGA) value which is larger than 0.1 s. The far-fault ground motions recorded at the same site at abovementioned earthquakes used to compare with near-fault ground motions.

2 Near-fault and far-fault ground motions

In this study, near-fault ground motion records are selected as an input ground motion from 1999 Chi-Chi, 1999 Kocaeli, and 1979 Imperial Valley earthquakes. These records are taken from station numbers TCU060, IZT180, and H-BRA225, respectively. In addition, another set of earthquake records, which recorded at the same site conditions from the same earthquakes events with epicenter far away from the site, is selected to illustrate far-fault ground motion characteristics. PGA and PGV, surface projection distances from the site to the fault, and PGV/PGA values are given in Table 1. The ground motion records are obtained from the PEER Strong Motion Database (PEER 2008). The database has information on the site conditions and the soil type for the instrument locations.

It is aimed to obtain two ground motion records with same peak acceleration values of each earthquake (1999 Chi-Chi, 1999 Kocaeli, and 1979 Imperial Valley) to compare the results more accurately. So, more attention was paid to the selection of records. If the ground motion records of each earthquake are selected randomly (different peak acceleration values), it cannot be said directly that near-fault ground motion has remarkable effects on the geometric nonlinear earthquake response of suspension bridges. So, it is aimed to eliminate this contradiction by selected ground motion records with same peak acceleration values.

The acceleration, velocity, and response spectra time-histories of the horizontal component of the near-fault and far-fault ground motions obtained from all earthquakes are shown in Figs. 2, 3, and 4, respectively. These figures show that the velocity pulses of the near-fault ground motions are significantly different as compared to the far-fault ground motions. The near-fault ground motions have significantly long-period velocity pulse.

The horizontal or longitudinal components of ground motions are important for an earthquake response analysis of many types of structures. For long-span bridges, however,

Table 1 Properties of selected near-fault and far-fault ground motion records

Ground motion	Earthquake	Station	PGA (m/s^2)	PGV (cm/s)	PGV/PGA (s)	M_w	Distance to fault (km)
Near fault	Chi-Chi	TCU060	0.20*g*	36.3	0.18	7.6	9.50
Far fault	Chi-Chi	ILA067	0.20*g*	11.8	0.06	7.6	48.68
Near fault	Kocaeli	IZT180	0.15*g*	22.6	0.15	7.8	4.80
Far fault	Kocaeli	FAT090	0.16*g*	0.09	0.06	7.8	64.50
Near fault	Imperial Valley	H-BRA225	0.16*g*	35.9	0.22	6.9	8.50
Far fault	Imperial Valley	H-CMP285	0.15*g*	9.5	0.06	6.9	32.60

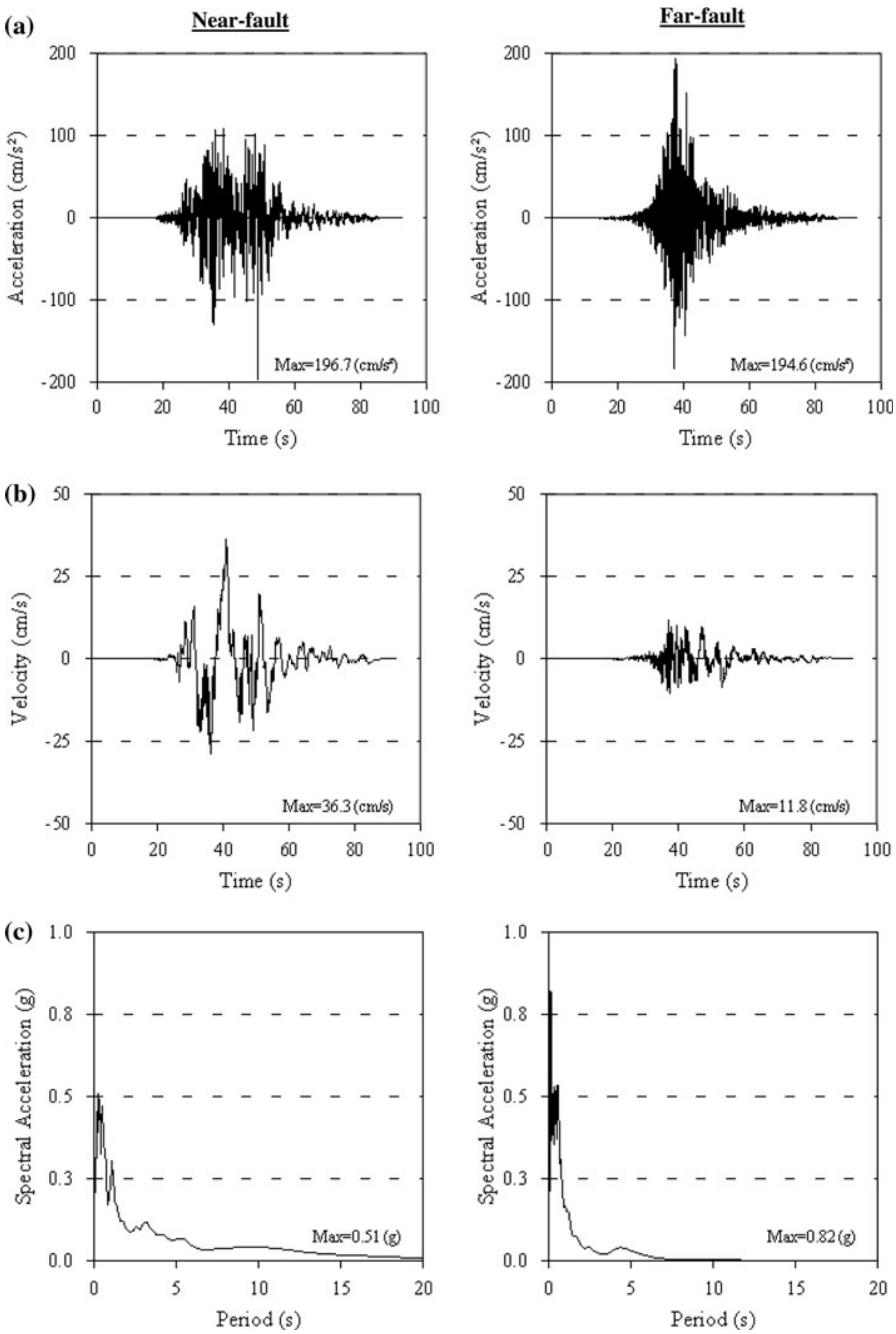

Fig. 2 Near-fault and far-fault ground motions recorded at 1999 Chi-Chi earthquake. **a** Acceleration time-histories for near-fault and far-fault ground motions. **b** Velocity time-histories for near-fault and far-fault ground motions. **c** Response spectra for near-fault and far-fault ground motions

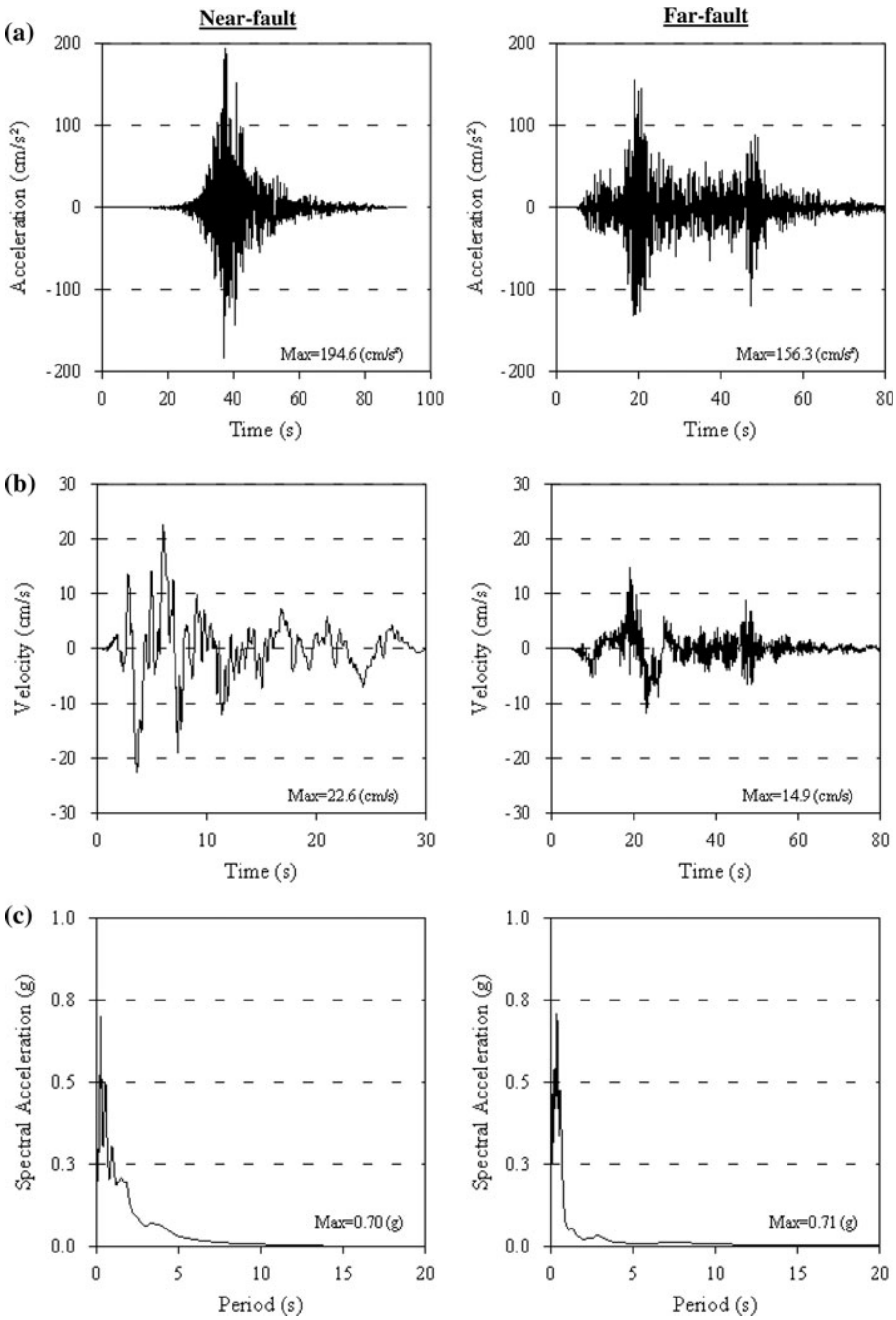

Fig. 3 Near-fault and far-fault ground motions recorded at 1999 Kocaeli earthquake. **a** Acceleration time-histories for near-fault and far-fault ground motions. **b** Velocity time-histories for near-fault and far-fault ground motions. **c** Response spectra for near-fault and far-fault ground motions

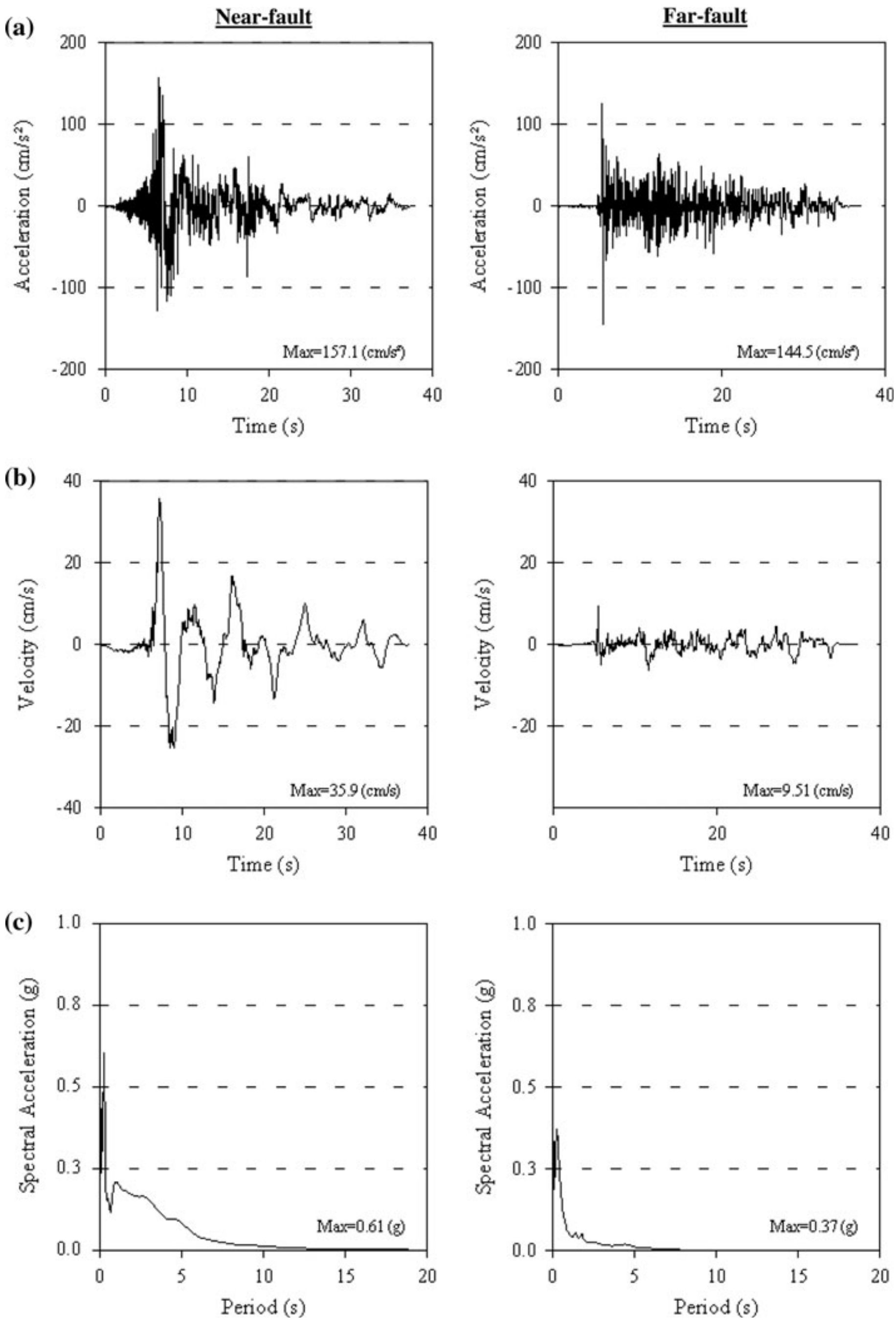

Fig. 4 Near-fault and far-fault ground motions recorded at 1979 Imperial Valley earthquake. **a** Acceleration time-histories for near-fault and far-fault ground motions. **b** Velocity time-histories for near-fault and far-fault ground motions. **c** Response spectra for near-fault and far-fault ground motions

vertical component of the ground motion is more important than lateral (longitudinal and transverse) components. Therefore, in this study, selected ground motion records are applied to only vertical direction, and lateral (longitudinal and transverse) motions are ignored (Abdel-Ghaffar and Stringfellow 1984; Dumanoğlu and Severn 1987, 1989).

3 Numerical examples

This study is focused on the determination and comparison of near-fault and far-fault strong ground motion effects on the geometrically nonlinear earthquake response of suspension bridges. Because of self-weight of suspension bridges, they have large displacements. These displacements cause geometric nonlinear behavior of suspension bridges. P-delta effect has significant effect on the numerical result for the present structural systems (Adanur 2003; Altunışık et al. 2006). The geometric nonlinearity due to self-weight of the bridges is taken into account, including the P-delta effects in the nonlinear dynamic analyses. 2D finite element models of the suspension bridges are prepared using the software SAP2000 (SAP2000 1998). The dimensional and material properties of the structural elements are selected by project drawings and calculation reports (Freeman et al. 1968; Brown and Parsons 1975). In this paper, the program is used to determine the dynamic characteristics and geometrically nonlinear behavior of bridges based on their physical and mechanical properties. Finite element models of the Boğaziçi and Fatih Sultan Mehmet suspension bridges have three degrees of freedom at each nodal point, namely two translational degrees of freedom in vertical and longitudinal axes and one rotational degree of freedom in lateral axis. As the deck, towers and cables are represented by beam elements, the hangers are represented by truss elements in the both bridges. The fact that this 2D model has relatively small number of degrees of freedom makes it more attractive by saving on computer time. Obviously, if actual design values for the responses are desired, 3D model should be taken into account. Although 2D bridge model includes some simplifications, it has been extensively used in the literature and has been shown to capture the dynamic behavior of 3D model. It was verified that 2D analysis provides natural frequencies and mode shapes which are in close agreement with those obtained by 3D analysis in the vertical direction for suspension bridges (Dumanoğlu and Severn 1985; Adanur 2003; Altunışık et al. 2006). Therefore, it is believed that the results based on the 2D analyses are representative of the actual 3D long-span bridge structures.

It is generally expected that finite element models based on technical design data and engineering judgments can yield reliable simulation for both the static and dynamic behaviors of suspension bridges. However, because of modeling uncertainties such as stiffness of supports and nonstructural elements, material properties and so on as well as inevitable differences between the properties of the designed and as-built structure, these finite element models often cannot predict natural frequencies and mode shapes with the required level of accuracy. This raises the need for verification of the finite element models of suspension bridges after their construction. For this purpose, modal testing is nowadays used commonly. The aim of modal testing is to determine as-built natural frequencies, mode shapes, and damping ratios. These are especially important when they are required to further study the behavior of suspension bridges.

There are two basically different methods available to experimentally identify the dynamic system parameters of a structure (of any kind, including suspension bridges): Experimental Modal Analysis and Operational Modal Analysis. In the Experimental Modal Analysis, the structure is excited by known input force (such as impulse hammers, drop

Table 2 The first 15 modal frequencies of the considered bridges

Mode number	Frequency (Hz)	
	First Bosporus bridge	Second Bosporus bridge
1	0.121	0.120
2	0.161	0.154
3	0.220	0.208
4	0.277	0.240
5	0.365	0.314
6	0.449	0.388
7	0.554	0.474
8	0.574	0.538
9	0.661	0.566
10	0.771	0.669
11	0.896	0.780
12	1.026	0.902
13	1.032	1.034
14	1.036	1.176
15	1.174	1.226

weights and electrodynamics shakers) and response of the structure is measured. In the Operational Modal Analysis, the structure is excited by unknown input force (ambient vibrations such as traffic load, wind and wave) and response of the structure is measured. Some heavy forced excitations become very expensive and sometimes may cause the possible damage to the structure. But ambient excitations such as traffic, wave, wind, earthquake and their combination are environmental or natural excitations. Therefore, the system identification techniques through ambient vibration measurements become very attractive. In this case, only response data of ambient vibrations are measurable while actual loading conditions are unknown. A system identification procedure will therefore need to base itself on output-only data. Ambient vibration tests using Operational Modal Analyses method were conducted on Boğaziçi and Fatih Sultan Mehmet Suspension Bridges to validate the finite element models (Dumanoğlu et al. 1989; Brownjohn et al. 1992).

Suspension bridges are not structurally homogeneous as building and dams. It was concluded from previous studies that the tower, deck, and cables affect the structural response in a wide range of modes (Dumanoğlu and Severn 1987). The number of modes plays a very important role in obtaining the acceptable results. Therefore, the first 15 modes of vibration and a 2 % of damping coefficient are adopted for the response calculations. The modal frequencies of the first fifteen modes of the bridges used in this study are given in Table 2. As can be seen from Table 2, the low modes of the both bridges have very low frequencies and are very closely spaces.

3.1 Earthquake response of Boğaziçi (First Bosporus) suspension bridge

The Boğaziçi (First Bosporus) suspension bridge (Fig. 5) (http://www.oib.gov.tr/portfoy/bogazici_koprusu.htm) connecting the Europe and Asia Continents in Istanbul, Turkey, is a 1,560 m long with a main span of 1,074 m and side spans of 231 and 255 m on the

Fig. 5 Picture of Boğaziçi (First Bosporus) Suspension Bridge (http://www.oib.gov.tr/portfoy/bogazici_koprusu.htm)

European and the Asian sides, respectively, without any side spans supported by cables. The decks of the side spans at the bridge are supported on the ground by piers. The bridge has flexible steel towers of 165 m high, inclined hangers and a steel box-deck. The horizontal distance between the cables is 28 m and the roadway is 21 m wide, accommodating three lanes each way. The roadway at the mid-span of the bridge is approximately 64 m above the sea level.

The 2D finite element model of the bridge with 202 nodal points, 199 beam elements and 118 truss elements is considered for the analyses. The selected finite element model of the bridge is represented by 475 degrees of freedom (Fig. 6). The material and section properties of the elements used in the finite element model are given in Table 3.

3.1.1 Tower responses

Time-histories of horizontal displacements at the top point of European side tower of Boğaziçi suspension bridge obtained from nonlinear analysis for near-fault and far-fault

Fig. 6 2D finite element model of Boğaziçi (First Bosporus) suspension bridge subjected to vertical ground motions

Table 3 Material and section properties of the elements of Boğaziçi Bridge

Elements	Material properties			
	Modulus of elasticity (kN/m^2)	Poisson's ratio (–)	Section areas (m^2)	Inertia moment (m^4)
Towers	2.05E8	0.30	1.360	9.0000
Deck	2.05E8	0.30	0.851	1.2380
Main cable	1.93E8	0.30	0.410	0.0133
Side span cable	1.93E8	0.30	0.438	0.0153
Hanger	1.62E8	0.30	0.0042	–

ground motions of 1999 Chi-Chi, 1999 Kocaeli, and 1979 Imperial Valley earthquakes are presented in Fig. 7. The maximum displacements on the tower occurred as 3.40–1.80 cm, 2.20–0.95 cm, and 5.50–1.02 cm for near-fault and far-fault ground motions, respectively. Figure 7 shows that maximum displacements occurred due to near-fault ground motions.

Variation in maximum horizontal displacements with height of European side tower for 1999 Chi-Chi, 1999 Kocaeli, and 1979 Imperial Valley earthquake ground motions is shown in Fig. 8. It can be seen from Fig. 8 that the horizontal displacements increase along the height of the tower and that those corresponding to near-fault ground motion are the highest.

Figure 9 points out the maximum internal forces such as bending moment, shear forces, and axial forces of the European side tower corresponding to the considering earthquake ground motions. It can be seen from Fig. 9 that all internal forces are the highest for the near-fault ground motions. Maximum bending moments occurred at the base of the tower for both near-fault and far-fault ground motions. The axial forces are nearly equal along the height of the tower, but the values of the shear forces are variable and maximum values come into being at the base of the tower.

3.1.2 Deck responses

The time-histories of vertical displacements at the middle point of the deck for both near-fault and far-fault ground motions of 1999 Chi-Chi, 1999 Kocaeli, and 1979 Imperial Valley earthquakes are presented in Fig. 10. The maximum displacements on the deck occurred as 56.1–31.9 cm, 31.2–12.0 cm, and 73.70–16.7 cm for near-fault and far-fault ground motions, respectively. Figure 10 shows that near-fault ground motions have effect on the deck displacements.

Variation in maximum displacements and bending moments along the deck for 1999 Chi-Chi, 1999 Kocaeli, and 1979 Imperial Valley earthquake ground motions is shown in Fig. 11. It can be seen from Fig. 11 that both maximum displacement and maximum bending moment values are obtained from the near-fault ground motion.

3.2 Earthquake response of Fatih Sultan Mehmet (Second Bosporus) suspension bridge

The Fatih Sultan Mehmet (Second Bosporus) suspension bridge (Fig. 12) (http://www.oib.gov.tr/portfoy/fatih_koprusu.htm) also connecting the Europe and Asia Continents in Istanbul, Turkey, has a box girder deck with 39.4 m wide overall and 1,090 m long. There are no side spans and the steel towers rise 110 m above the ground level. The hangers are

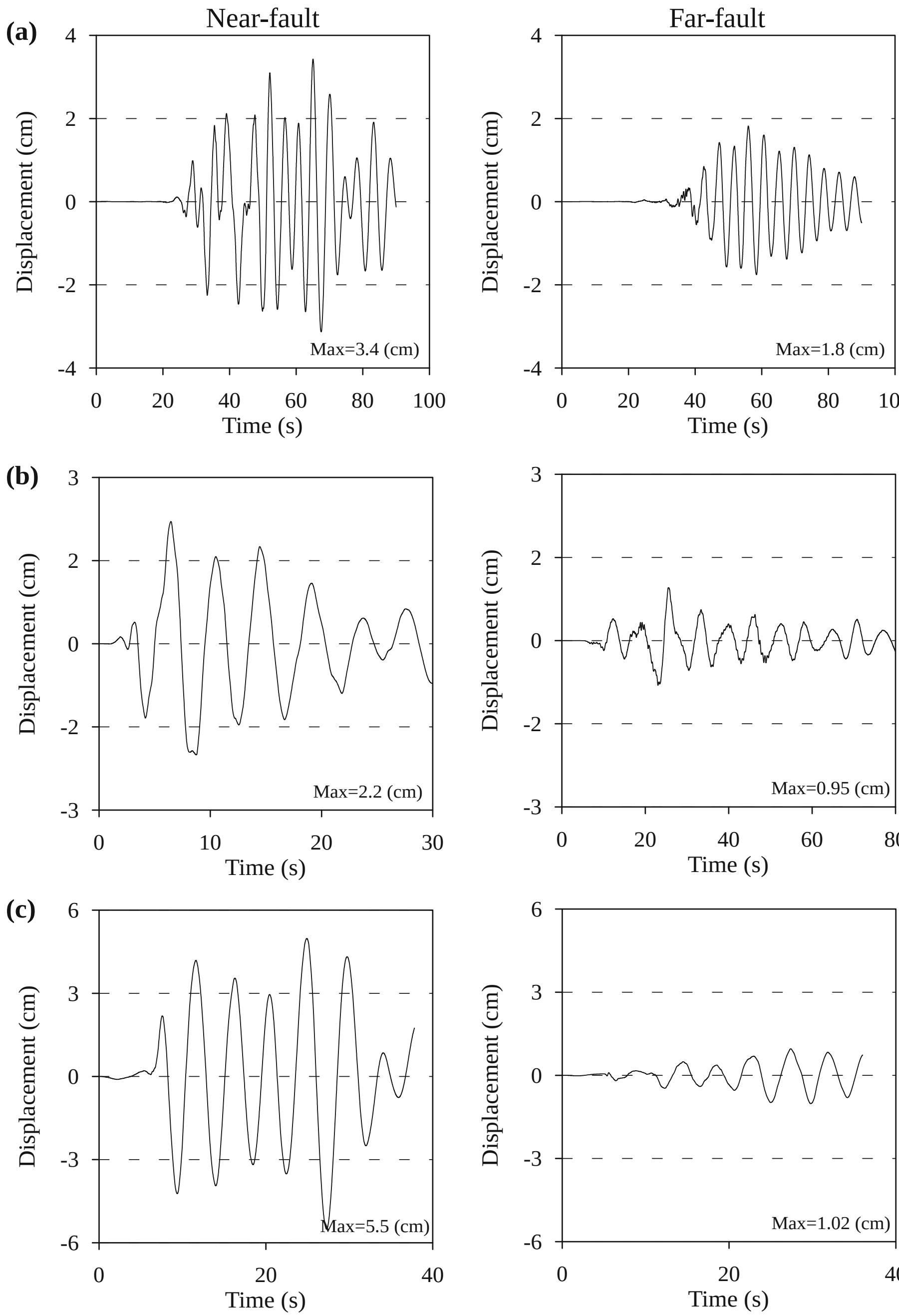

Fig. 7 Time-histories of horizontal displacements at the top of the European side tower of Boğaziçi suspension bridge. **a** Time-histories of horizontal displacements for 1999 Chi-Chi earthquake. **b** Time-histories of horizontal displacements for 1999 Kocaeli earthquake. **c** Time-histories of horizontal displacements for 1979 Imperial Valley earthquake

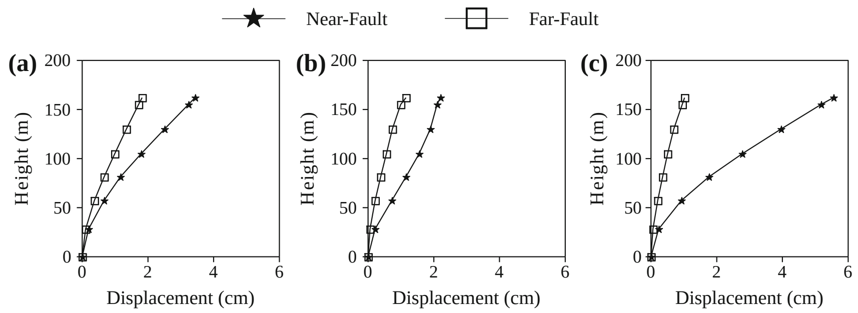

Fig. 8 Maximum horizontal displacements along the height of European side tower of Boğaziçi suspension bridge. **a** 1999 Chi-Chi, **b** 1999 Kocaeli, **c** 1979 Imperial Valley

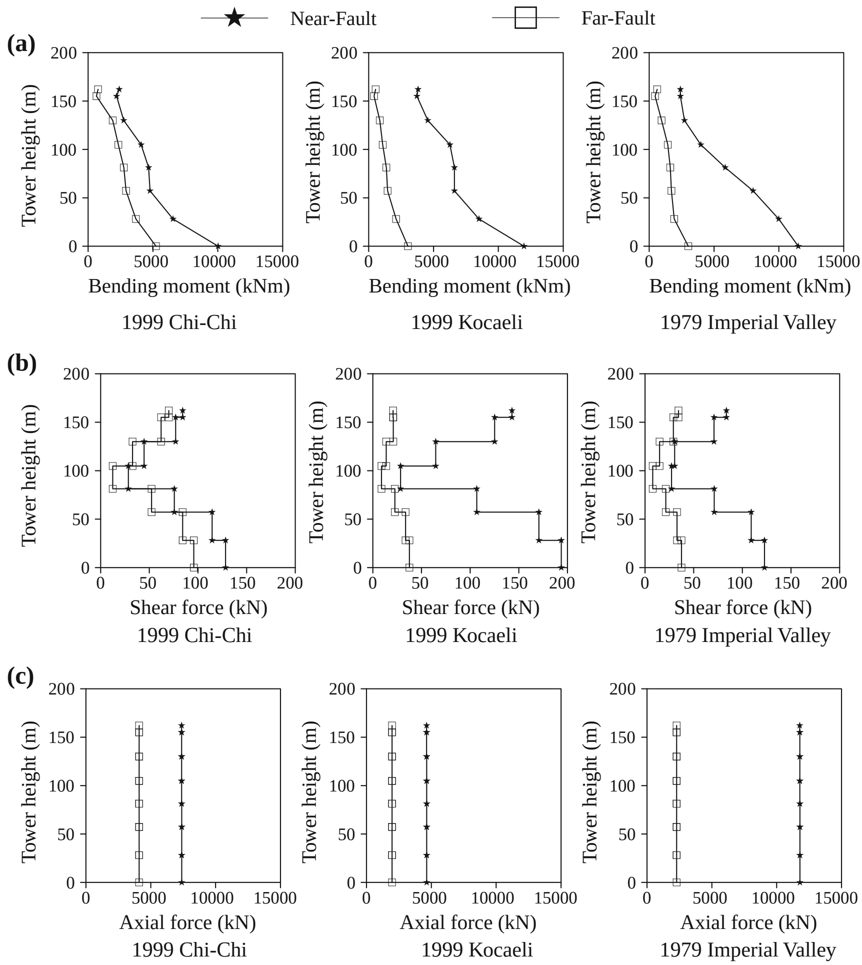

Fig. 9 Maximum bending moments (**a**), shear forces (**b**), and axial forces (**c**) at the European side tower of Boğaziçi suspension bridge

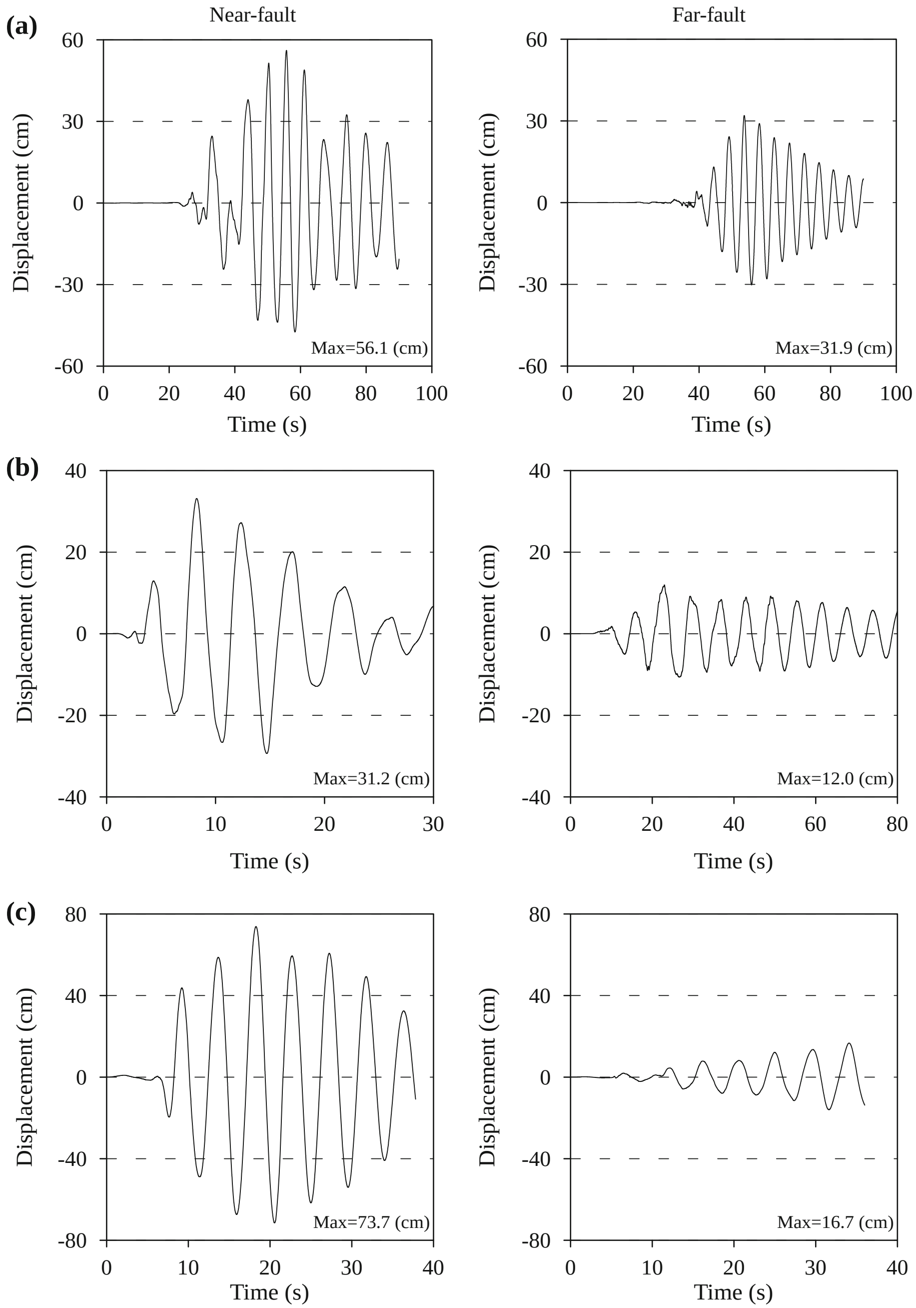

Fig. 10 Time-histories of vertical displacements on the deck of Boğaziçi suspension bridge. **a** Time-histories of vertical displacements for 1999 Chi-Chi earthquake. **b** Time-histories of vertical displacements for 1999 Kocaeli earthquake. **c** Time-histories of vertical displacements for 1979 Imperial Valley earthquake

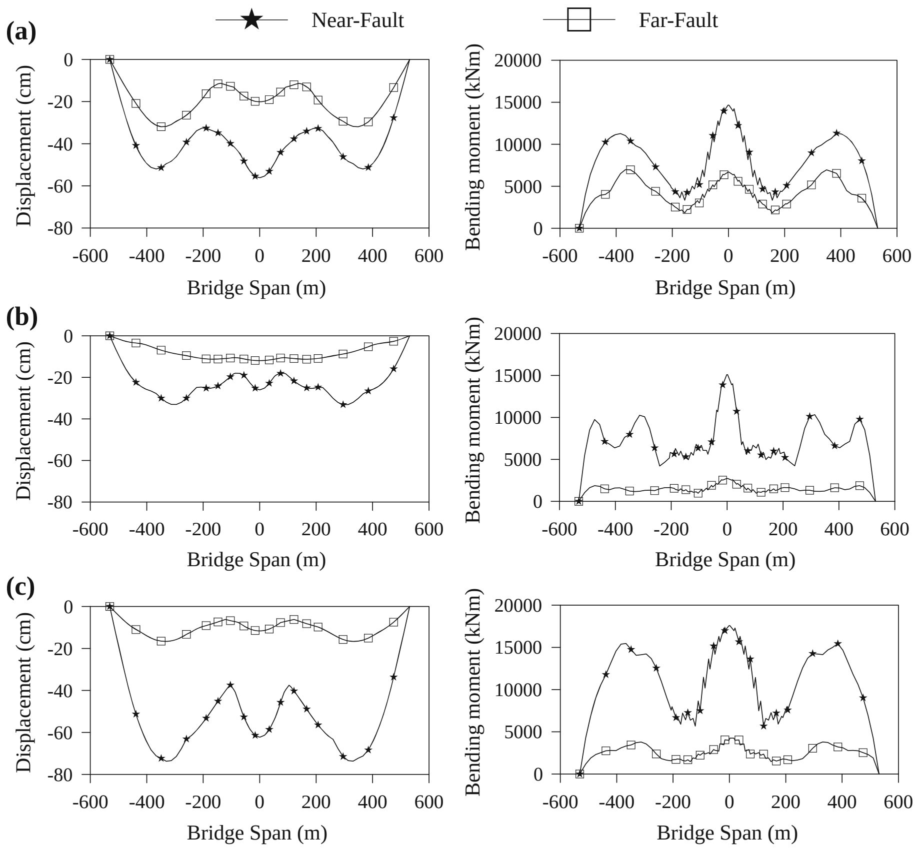

Fig. 11 Dynamic response values of Boğaziçi suspension bridge deck. **a** Displacement and bending moment subjected to 1999 Chi-Chi earthquake. **b** Displacement and bending moment subjected to 1999 Kocaeli earthquake. **c** Displacement and bending moment subjected to 1979 Imperial Valley earthquake

vertical and connected to the deck and cable with singly hinged bearing. The horizontal distance between the cables is 33.8 m and the roadway is 28 m wide, accommodating two four-lane highways. The roadway at the mid-span of the bridge is approximately 64 m above the sea level.

The 2D finite element model of the bridge with 144 nodal points, 142 beam elements, 60 truss elements is used in the analyses. The finite element model of the bridge has 418 degrees of freedom (Fig. 13). The material and section properties of the elements used in the finite element model are given in Table 4.

3.2.1 Tower responses

Time-histories of horizontal displacements at the top point of European side tower of Fatih Sultan Mehmet suspension bridge obtained from nonlinear analysis for near-fault and far-fault ground motions of 1999 Chi-Chi, 1999 Kocaeli, and 1979 Imperial Valley earthquakes are presented in Fig. 14. The maximum displacements on the tower occurred as

Fig. 12 Picture of Fatih Sultan Mehmet (Second Bosporus) Suspension Bridge (http://www.oib.gov.tr/portfoy/fatih_koprusu.htm)

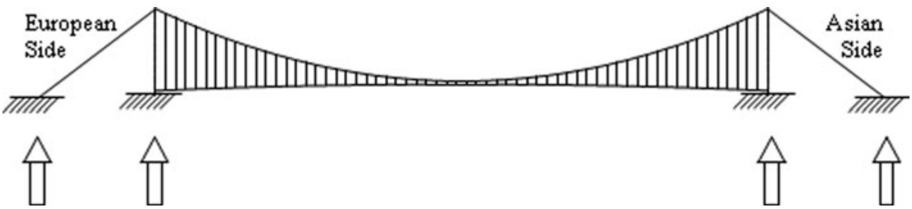

Fig. 13 2D finite element model of Fatih Sultan Mehmet (Second Bosporus) suspension bridges subjected to vertical ground motions

Table 4 Material and section properties of the elements of Fatih Sultan Mehmet Bridge

Element	Material properties			
	Modulus of elasticity (kN/m^2)	Poisson's ratio (–)	Section areas (m^2)	Inertia moment (m^4)
Towers	2.05E8	0.30	2.68	6.4100
Deck	2.05E8	0.30	1.26	1.7300
Main cable	1.93E8	0.30	0.7333	0.0428
Side span cable	1.93E8	0.30	0.7835	0.0488
Hanger	1.62E8	0.30	0.0181	–

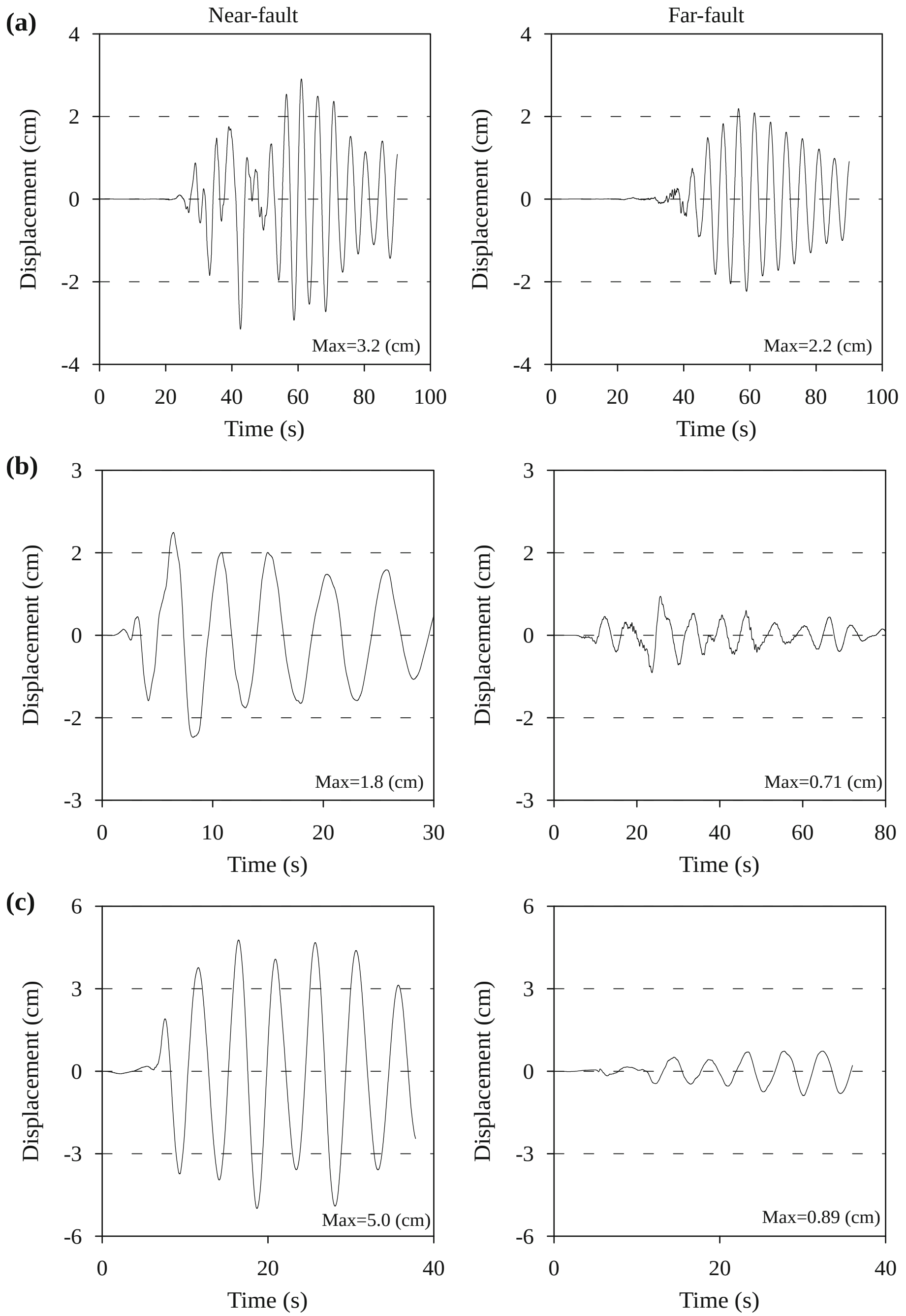

Fig. 14 Time-histories of horizontal displacements at the top of the European side tower of Fatih Sultan Mehmet suspension bridge. **a** Time-histories of horizontal displacements for 1999 Chi-Chi earthquake. **b** Time-histories of horizontal displacements for 1999 Kocaeli earthquake. **c** Time-histories of horizontal displacements for 1979 Imperial Valley earthquake

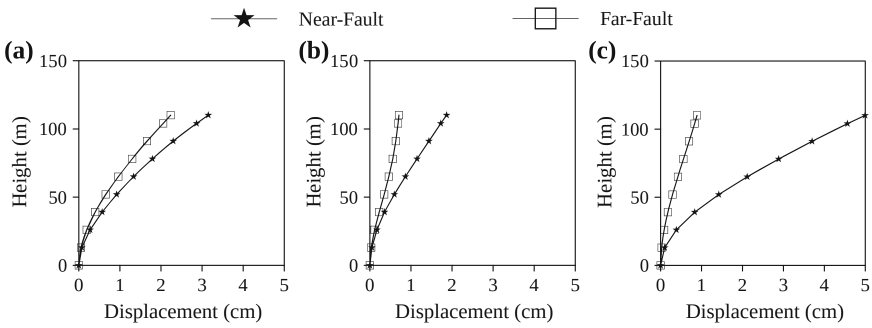

Fig. 15 Maximum horizontal displacements along the height of European side tower of Fatih Sultan Mehmet suspension bridge. **a** 1999 Chi-Chi, **b** 1999 Kocaeli, **c** 1979 Imperial Valley

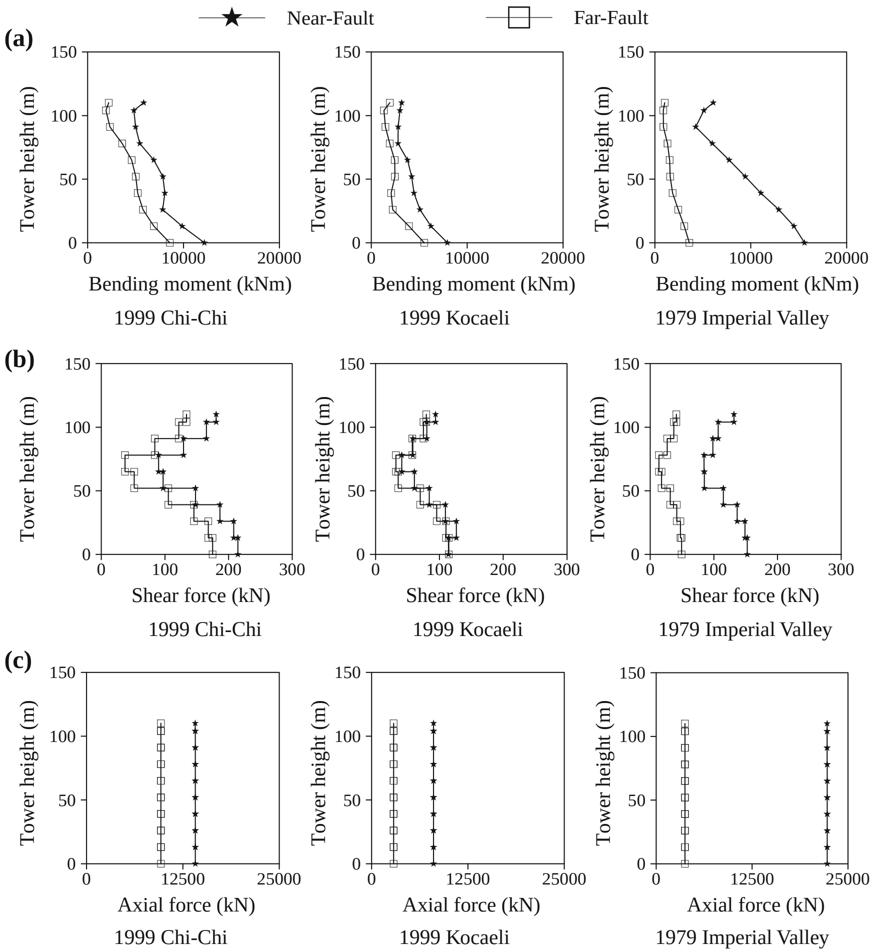

Fig. 16 Maximum bending moments (**a**), shear forces (**b**), and axial forces (**c**) at the European side tower of Fatih Sultan Mehmet suspension bridge

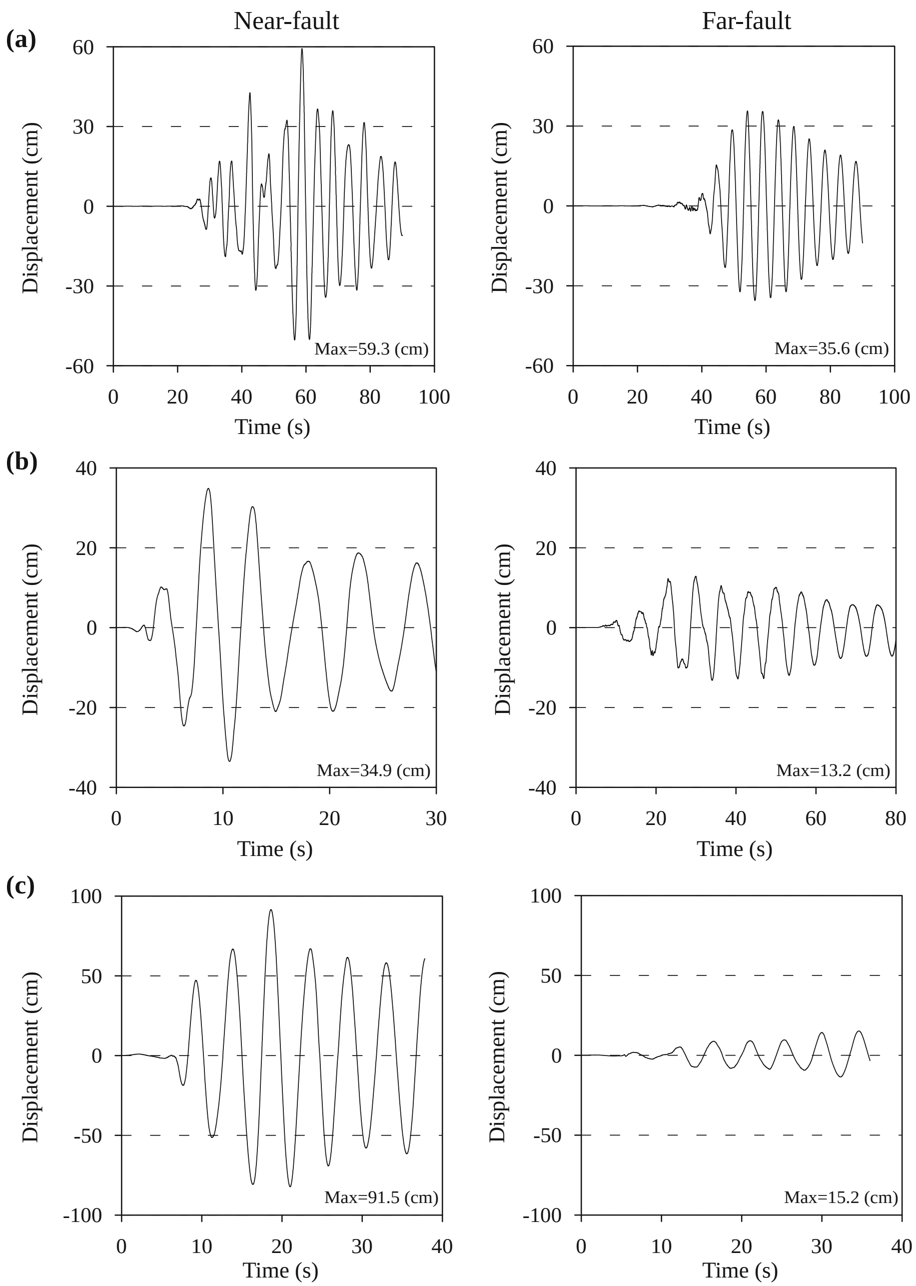

Fig. 17 Time-histories of vertical displacements on deck of Fatih Sultan Mehmet suspension bridge. **a** Time-histories of vertical displacements for 1999 Chi-Chi earthquake. **b** Time-histories of vertical displacements for 1999 Kocaeli earthquake. **c** Time-histories of vertical displacements for 1979 Imperial Valley earthquake

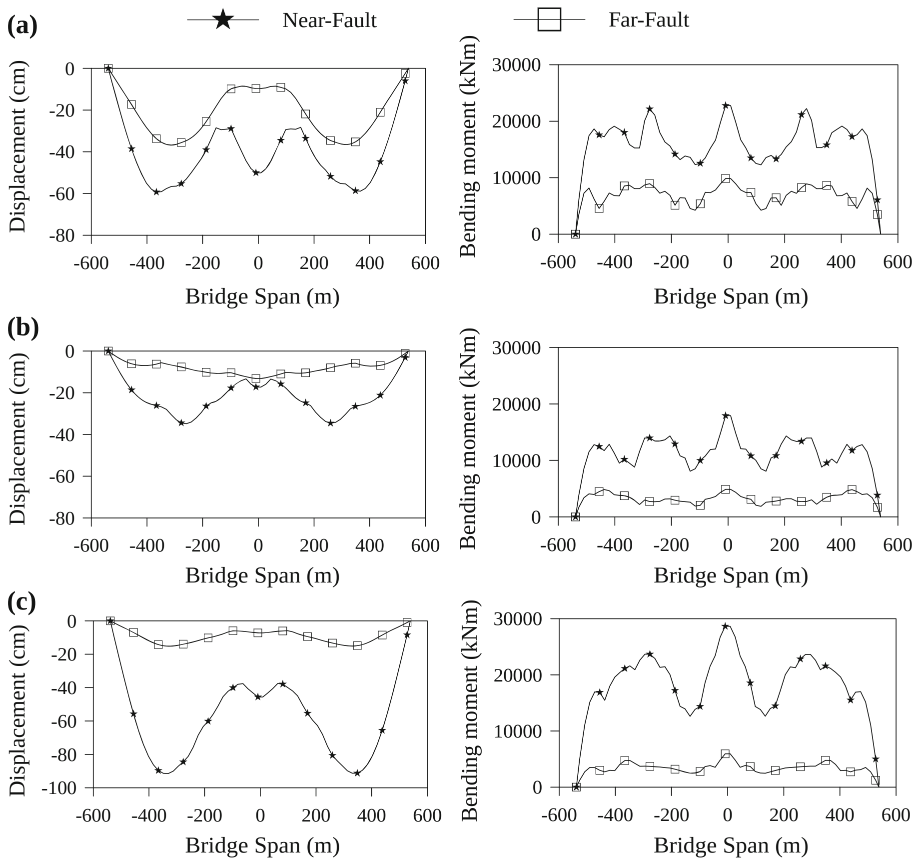

Fig. 18 Dynamic response values of Fatih Sultan Mehmet suspension bridge deck. **a** Displacement and bending moment subjected to 1999 Chi-Chi earthquake. **b** Displacement and bending moment subjected to 1999 Kocaeli earthquake. **c** Displacement and bending moment subjected to 1979 Imperial Valley earthquake

3.2–2.2 cm, 1.8–0.71 cm, and 5.0–0.89 cm for near-fault and far-fault ground motions, respectively. Figure 14 shows that maximum displacements occurred due to near-fault ground motions.

Variation in maximum horizontal displacements with height of European side tower for 1999 Chi-Chi, 1999 Kocaeli, and 1979 Imperial Valley earthquake ground motions is shown in Fig. 15. It can be seen from Fig. 15 that the horizontal displacements increase along the height of the tower and that those corresponding to near-fault ground motion are the highest.

Figure 16 points out the maximum internal forces such as bending moment, shear forces, and axial forces of the European side tower corresponding to all earthquake ground motions. It can be seen from Fig. 16 that all internal forces are the highest for the near-fault ground motion. The values of the axial forces are nearly equal along the height of the tower, but the values of the shear forces are variable and maximum values come into being at the base of the tower. Also, maximum bending moments occurred at the base of the tower for both near-fault and far-fault ground motion records.

3.2.2 Deck responses

The time-histories of vertical displacements at the middle point of the deck for both near-fault and far-fault ground motions of 1999 Chi-Chi, 1999 Kocaeli, and 1979 Imperial Valley earthquakes are presented in Fig. 17. The maximum displacements on the deck occurred as 59.3–35.6 cm, 34.9–13.2 cm, and 91.5–15.2 cm for near-fault and far-fault ground motions, respectively. Figure 17 shows that near-fault ground motions have effect on the deck displacements.

Variation in displacements and bending moments along the deck for 1999 Chi-Chi, 1999 Kocaeli, and 1979 Imperial Valley earthquake ground motions is shown in Fig. 18. It can be seen from Fig. 18 that both maximum displacements and maximum bending moment values occurred under the near-fault ground motion records.

4 Conclusions

This paper presents a comparison of near-fault and far-fault ground motion effects on geometrically nonlinear earthquake behavior of suspension bridges. Boğaziçi (The First Bosporus) and Fatih Sultan Mehmet (Second Bosporus) suspension bridges built in Istanbul, Turkey, are selected as numerical examples. Geometric nonlinearity including P-delta effects from self-weight of the bridges is considered in the determination of the dynamic behavior of the suspension bridges for near-fault and far-fault ground motions.

While displacements along the height of the tower have an increasing trend, bending moments have a decreasing trend for both suspension bridges. In addition to these, axial forces are nearly constant along the tower, but shear forces values are variable. Along the suspension deck, maximum bending moments occurred at the middle point of the deck but maximum displacements are variable for Boğaziçi and Fatih Sultan Mehmet suspension bridges.

The performed geometric nonlinear analyses showed that near-fault ground motion is rather effective on the displacements and internal forces in the suspension bridges. The maximum displacements and maximum internal forces from the suspension bridges obtained for near-fault ground motion are effective than those for far-fault ground motion. It should be clarified that the near-fault ground motion effects appear along the duration of earthquake. It is also seen that maximum displacements and internal forces have not occurred when near-fault ground motions have peak acceleration value.

According to this study, near-fault earthquake ground motion has remarkable effects on the geometric nonlinear response of suspension bridges. In the next studies related to earthquake responses of engineering structures such as suspension bridges, near-fault ground motion effects should be taken into account to obtain more realistic results.

References

Abdel-Ghaffar AM (1976) Dynamic analyses of suspension bridge structures. EERL 76-01, California Institute of Technology, Pasadena

Abdel-Ghaffar AM (1980) Vertical vibration analysis of suspension bridges. J Struct Div 106:2053–2074

Abdel-Ghaffar AM, Rubin LI (1982) Suspension bridge response to multiple-support excitations. J Eng Mech 108:419–435
Abdel-Ghaffar AM, Rubin LI (1983a) Nonlinear free vibrations of suspension bridges. J Eng Mech 109:313–345
Abdel-Ghaffar AM, Rubin LI (1983b) Vertical seismic behaviour of suspension bridges. Earthq Eng Struct Dyn 11:1–19
Abdel-Ghaffar AM, Stringfellow RG (1984) Response of suspension bridges to travelling earthquake excitations. Soil Dyn Earthq Eng 3:62–81
Adanur S (2003) Geometrically nonlinear deterministic and stochastic analyses of suspension bridges to multiple support seismic excitations. PhD Thesis, Karadeniz Technical University, Trabzon
Agrawal AK, He WL (2002) A closed-form approximation of near-fault ground motion pulses for flexible structures. In: 15th ASCE engineering mechanics conference, New York
Akkar S, Yazgan U, Gulkan P (2005) Drift estimates in frame buildings subjected to near-fault ground motions. J Struct Eng ASCE 131:1014–1024
Altunışık AC, Bayraktar A, Adanur S (2006) Effect of hanger shapes on the geometric nonlinear static and dynamic responses of Bosporus suspension bridge. In: 17th International congress on advances in civil engineering, İstanbul
Archuleta RJ, Hartzell SH (1981) Effect of fault finiteness on near-source ground motion. Bull Seismol Soc Am 71:939–957
Bayraktar A, Altunisik AC, Sevim B, Kartal ME, Turker T (2008) Near-fault ground motion effects on the nonlinear response of dam-reservoir-foundation systems. Struct Eng Mech 28:11–42
Bray JD, Marek AR (2004) Characterization of forward-directivity ground motions in the near-fault region. Soil Dyn Earthq Eng 24:815–828
Brown WC, Parsons MF (1975) Bosporus Bridge, part 1: history of design. Proc Inst Civ Eng 1(58):505–532
Brownjohn JMW (1994) Observations on non-linear dynamic characteristics of suspension bridges. Earthq Eng Struct Dyn 23:1351–1367
Brownjohn JMW, Dumanoğlu AA, Severn RT (1992) Ambient vibration survey of the Fatih Sultan Mehmet suspension bridge. Earthq Eng Struct Dyn 21:907–924
Chopra AK, Chintanapakdee C (2001) Comparing response of SDF systems to near-fault and far-fault earthquake motions in the context of spectral regions. Earthq Eng Struct Dyn 30:1769–1789
Corigliano M, Lai CG, Barla G (2006) Seismic response of rock tunnels in near-fault conditions. In: 1st European conference on earthquake engineering and seismology, Switzerland
Dicleli M, Buddaram S (2007) Equivalent linear analysis of seismic-isolated bridges subjected to near-fault ground motions with forward rupture directivity effect. Eng Struct 29:21–32
Dumanoğlu AA, Severn RT (1985) Asynchronous seismic analysis of modern suspension bridges. Part 1: Free vibration, Department of Civil Engineering, University of Bristol, Bristol
Dumanoğlu AA, Severn RT (1987) Seismic response of modern suspension bridges to asynchronous vertical ground motion. Proc Inst Civ Eng 83:701–730
Dumanoğlu AA, Severn RT (1989) Seismic response of modern suspension bridges to asynchronous longitudinal and lateral ground motion. Proc Inst Civ Eng 87:73–86
Dumanoğlu AA, Severn RT (1990) Stochastic response of suspension bridges to earthquake forces. Earthq Eng Struct Dyn 19:133–152
Dumanoğlu AA, Brownjohn JMW, Severn RT, Blakeborough A (1989) Ambient vibration survey of the bosporus suspension bridge. Earthq Eng Struct Dyn 18:263–283
Dumanoğlu AA, Brownjohn JMW, Severn RT (1992) Seismic analysis of the Fatih Sultan Mehmet (Second Bosporus) Suspension Bridge. Earthq Eng Struct Dyn 21:881–906
Freeman, Fox and Partners (1968) Bosporus bridge calculations. Westminster, London, S.W.I
Galal K, Ghobarah A (2006) Effect of near-fault earthquakes on North American nuclear design spectra. Nucl Eng Des 236:1928–1936
Ghahari F, Jahankhah H, Ghannad MA (2006) The effect of background record on response of structures subjected to near-fault ground motions. In: 1st European conference on earthquake engineering and seismology, Switzerland
Hall JF, Heaton TH, Halling MW, Wald DJ (1995) Near-source ground motion and its effects on flexible buildings. Earthq Spectra 11:569–605
Harichandran RS, Hawwari A, Sweiden BN (1996) Response of long-span bridges to spatially varying ground motion. J Struct Eng 122:476–484
Hyun CH, Yun CB, Lee DG (1992) Nonstationary response analysis of suspension bridges for multiple support excitations. Prob Eng Mech 7:27–35
Liao WI, Loh CH, Lee BH (2004) Comparison of dynamic response of isolated and non-isolated continuous girder bridges subjected to near-fault ground motions. Eng Struct 26:2173–2183

Malhotra PK (1999) Response of buildings to near-fault pulse-like ground motions. Earthq Eng Struct Dyn 28:1309–1326
Megawati K, Higashihara H, Koketsu K (2001) Derivation of near-source ground motions of the 1995 Kobe (Hyogo-ken Nanbu) earthquake from vibration records of the Akashi Kaikyo Bridge and its implications. Eng Struct 23:1256–1268
Nakamura Y, Der Kiureghian A, Liu D (1993) Multiple-support response spectrum analysis of the Golden Gate Bridge. Report No. UCB/EERC-93/05, Berkeley (CA), Earthquake Engineering Research Center, College of Engineering, University of California
Ohmachi T, Jalali A (1999) Fundamental study on near-fault effects on earthquake response of arch dams. Earthq Eng Eng Seismol 1:1–11
PEER (2008) http://peer.berkeley.edu/smcat/data. Accessed 13 March 2008
Pulido N, Kubo T (2004) Near-fault strong motion complexity of the 2000 Tottori earthquake (Japan) from a broadband source asperity model. Tectonophysics 390:177–192
Rao BP, Jangid RS (2001) Performance of sliding systems under near-fault motions. Nucl Eng Des 203:259–272
Rassem M, Ghobarah A, Heidebrecht AC (1996) Site effects on the seismic response of a suspension bridge. Eng Struct 18:363–370
SAP2000 (1998) Integrated finite element analysis and design of structures. Computers and Structures Inc., Berkeley
Somerville PG (2003) Magnitude scaling of the near fault rupture directivity pulse. Phys Earth Planet Int 137:201–212
Wang J, Hu S, Wei X (1999) Effects of engineering geological condition on response of suspension bridges. Soil Dyn Earthq Eng 18:297–304
Wang GQ, Zhou XY, Zhang PZ, Igel H (2002) Characteristics of amplitude and duration for near fault strong ground motion from the 1999 Chi-Chi, Taiwan earthquake. Soil Dyn Earthq Eng 22:73–96
Zhang YH, Lin JH, Williams FW, Li QS (2005) Wave passage effect of seismic ground motions on the response of multiply supported structures. Struct Eng Mech 20:655–672